

Dynamic distribution and tissue tropism of avian encephalomyelitis virus isolate XY/Q-1410 in experimentally infected Korean quail

Lili Fan¹ · Zhijun Li¹ · Jiali Huang¹ · Zengqi Yang¹ · Sa Xiao¹ · Xinglong Wang¹ · Ruyi Dang¹ · Shuxia Zhang¹

Received: 18 January 2017 / Accepted: 20 June 2017 / Published online: 9 August 2017
© Springer-Verlag GmbH Austria 2017

Abstract Avian encephalomyelitis (AE) is an important infectious poultry disease worldwide that is caused by avian encephalomyelitis virus (AEV). However, to date, the dynamic distribution of AEV in quails has not been well described. Quantitative real-time polymerase chain reaction (qPCR) and immunohistochemistry (IHC) assays were used to investigate the dynamic distribution and tissue tropism of AEV in experimentally infected Korean quail. AEV was detected in the cerebrum, cerebellum, proventriculus, intestine, liver, pancreas, spleen, bursa, lung and kidney as early as 3 days post-infection (dpi). The viral loads in the proventriculus, intestine, spleen and bursa were relatively higher than in other tissues. According to the qPCR results, AEV XY/Q-1410 infection lasted for at least 60 days in infected Korean quail. Immunohistochemistry-positive staining signals of AEV antigen were analysed by Image-Pro Plus software. A positive correlation between qPCR and IHC results was identified in most tissues. Our results provide an insight into the dynamic distribution of AEV in various tissues after infection. The distinct dynamic distribution of the viral genome in Korean quail in the early and late stages of infection suggests that AEV replication is affected by antibody levels and the maturity of the immune system of the host.

Introduction

Avian encephalomyelitis (AE), which is caused by avian encephalomyelitis virus (AEV), is an important poultry infectious disease of chicken, pheasant, turkey and quail worldwide [1–3]. Young chicks show neurological symptoms, including ataxia, paresis and rapid tremors of the head and neck, and have high morbidity and variable mortality [4]. In adult chickens, infection is usually subclinical, although accompanied by transient declines in egg production and hatchability [5–8].

AEV viruses (classified within the family *Picornaviridae* within the genus *Tremovirus*) are non-enveloped, single-stranded and positive-sense RNA viruses [1, 9, 10]. As AEV does not grow efficiently with a low titre and has no visible cytopathic effect in cell culture [11–13], the detection of AEV is limited to specific antibody assays, such as neutralisation [14], serum-neutralisation [15], agar gel precipitation [16], fluorescent antibody [17, 18] and passive haemagglutination [19] tests. Molecular biology techniques, such as RT-PCR, cDNA hybridisation probes, and quantitative real-time PCR (qPCR), are capable of more rapid and sensitive detection of AEV than antibody-based methods and qPCR has been used to detect the virus genome and quantify the viral RNA [4].

To date, the tissue distribution of AEV has only been conducted in experimentally infected chickens or laying hens using fluorescent antibody tests [20, 21]. No study on the tissue distribution of AEV in quails has ever been published. Recently, several clinical cases have indicated that AE in quail farms can result in losses, due to the death of quails. However, the pathogenic mechanisms underpinning AEV mortality in quails is not clear. As the knowledge of virus distribution within an infected host is essential for understanding the pathogenic mechanisms of the virus, we

Electronic supplementary material The online version of this article (doi:10.1007/s00705-017-3504-0) contains supplementary material, which is available to authorized users.

✉ Shuxia Zhang
zhangshuxia316316@163.com

¹ College of Veterinary Medicine, Northwest A&F University, Yangling 712100, Shaanxi, China

analysed the dynamic tissue distribution of AEV at the very early stage of infection. These data may also provide useful information for AEV detection and control.

Materials and methods

Virus preparation

The AEV isolate XY/Q-1410 (KY454766) was collected from naturally infected quails from Xianyang in 2014. Infections by several other avian viruses (NDV, IBV, AIV (H9N2)) were ruled out by PCR detection. The methods for detection were as described as previously [22–24]. The results are also shown in the supplementary material (Fig. S1). Virus in homogenate –0.2 g of infected quail brain in 200 μ l of cold phosphate-buffered saline (PBS) was titred to calculate the median embryo infectious dose (EID₅₀). The EID₅₀ was calculated according to the algorithm of the Reed–Muench method [25]. The grinding fluid was stored at –80 °C until use.

Challenge experiments and sampling

Two hundred one-day-old Korean quails were randomly separated into two groups: the non-infected group (group I, n = 80) and the infected group (group II, n = 120). All the quails were maintained in isolators and fed a commercial diet twice per day. Each bird in group II was challenged with 10⁵ EID₅₀/0.2 ml of XY/Q-1410 (diluted homogenate) orally while control birds in group I were orally given 0.2 ml PBS. Three quails from group II and two from group I were euthanised by cervical dislocation for sample collection at days: 3–17 (one-day intervals), 18–25 (every day), 29, 30, 32, 36–48 (one-day intervals), 49 and 51–60 (every day) days post-infection (dpi), respectively. Organs (cerebrum, cerebellum, proventriculus, intestine, liver, pancreas, spleen, bursa, lungs and kidneys) were aseptically collected at each interval for virus detection by qPCR and immunohistochemistry (IHC).

All the animal experiments were approved by the Ethical and Animal Welfare Committee of Northwest A&F University, Shaanxi, China.

RNA extraction and cDNA synthesis

Total RNA was extracted from the homogenate of 200 mg of tissues in 400 μ l PBS using the RNAiso plus reagent kit (TaKaRa, Dalian, China) and the manufacturer's instructions and then stored at –80 °C until use. The first-strand cDNA synthesis was carried out according to the HiScript® Q RT SuperMix for qPCR (Vazyme, Nanjing, China.) in a 10- μ l reaction volume containing 1 μ g total RNA and 2 μ l 5 \times qRT

SuperMix. The reverse transcription reaction was conducted in a PCR machine as follows: 25 °C for 10 min, 50 °C for 30 min, 45 °C for 5 min, and then 4 °C indefinitely. The cDNA was stored at –20 °C until use.

Quantitative real-time polymerase chain reaction assay (qPCR)

A standard curve was established with serially diluted plasmids (10²–10⁸ copies/ μ l) that harboured the VP1 gene of AEV. The PCR product size was 288 bp while the primers have been reported previously [4]. The TIANLONG 988 Real-Time PCR System (Xian, China) was used to generate the standard curve. qPCR detection was performed in triplicate for each sample independently in a 20 μ l reaction mixture containing 10 μ l Ultra SYBR Mixture (CW Biotech, China), 0.4 μ l each primer (10 μ M), and 2 μ l cDNA or distilled water (blank control). The reactions were performed using an Ultra SYBR Mixture thermocycler at 95 °C for 10 min, followed by 40 cycles of 95 °C for 15 s, 55 °C for 30 s, and 72 °C for 50 s. Fluorescence was measured by a program set up in advance. Absolute quantification of viral copies was determined by comparison with the standard curve. A melting curve analysis was used to evaluate the amplification result.

Immunohistochemical (IHC) detection

The cerebrum, cerebellum, proventriculus, intestine, liver, pancreas, spleen, bursa, lung and kidney from challenged quails collected at 7, 18, 36, 54 and 59 dpi was used for IHC analysis with a protocol that was reported previously [26]. Briefly, 5- μ m paraffin-embedded sections were deparaffinized and rehydrated, the viral antigen was retrieved, endogenous peroxidase was eliminated and the sections were blocked. The sections were incubated with a specific primary antibody diluted 1:20 for 1 h at 37 °C. After being rinsed, sections were incubated with biotinylated goat anti-rabbit IgG and streptavidin-conjugated HRP (Bioss Biotech, China). Subsequently, the sections were stained with diaminobenzidine (CW Biotech, China) and then counterstained with haematoxylin. In the negative controls, the primary antibody was replaced with PBS. The immunohistochemical staining of viral antigen was analysed using Image-Pro Plus (IPP) 6.0 software (Media Cybernetics, Bethesda, USA) using the method described in [27]. Briefly, three digital images at 1024 \times 768 pixel resolution and 400 \times magnification were captured by the Motic BA210LED Digital (Motic, Hong Kong). The measurement parameters included IOD, area sum and mean density. The optical density was calibrated and the area of interest (AOI) was set as follows: hue, 0–30; saturation, 0–255; intensity, 0–255. The image

was then converted to a greyscale image and the values were measured.

Statistical analysis

The Statistical Product and Service Solutions (SPSS) software (version 16.0; International Business Machines Corporation, Armonk, USA) was used for statistical analysis. The values of viral RNA and viral antigen are presented as the mean \pm standard deviation (SD). Significant differences in viral load were analysed by one-way ANOVA with Dunnett's T3 test. The correlation between viral RNA calculated from the standard curve of the qPCR assay and the viral antigen estimated by IHC was analysed using Kendall's tau-b, two-tailed test. The pictures were assembled using Adobe Photoshop CS software (version 6.0; San Jose, USA).

Results

Clinical observation

Slight depression of quails was observed at 10 dpi in the infected group. Hypokinesia and dullness were apparent at 16 dpi. Six quails kneeled down and walked on their tarsal joints at 17 dpi. The typical clinical symptoms of AEV, including paralysis and tremors of the head and neck, were observed at 18 dpi and these quails had died within one hour after the typical clinical symptoms appeared. The first death and the highest number of deaths occurred at 18 dpi. The morbidity was 30% and the mortality was 16.7%. In the surviving birds, the clinical symptoms gradually disappeared from 25 dpi and the remaining quails seemed quite healthy. No clinical symptoms were observed in the non-infected group.

Distribution of AEV in different tissues

The standard curve demonstrated a strong correlation between the number of templates and the Ct value. The reaction efficiency was 99.87%. The slope of the standard curve was -3.325 and the correlation coefficient (R^2) was 0.9978. The lower detection limit was about 100 copies however the repeatability was not acceptable when the number of templates decreased to ten copies.

The viral RNA in the cerebrum, cerebellum, proventriculus, intestine, liver, pancreas, spleen, bursa, lung and kidney tissues of infected quails was quantified by referring to the standard curve. Viral RNA was detected in the tissues at 3 dpi with a virus load ranging from 1.06×10^2 to 6.92×10^6 copies/ μ L (Fig. 1). The AEV viruses were detectable in most tissues until 60 dpi.

In the cerebrum and cerebellum, the viral load was relatively stable and fluctuated only slightly. Consistent with the early clinical symptoms, the first viral load peak point appeared at 18 dpi (4.07×10^2 copies/ μ L in the cerebrum and 1.62×10^4 copies/ μ L in the cerebellum, $P < 0.001$) and, surprisingly, another peak with an even higher viral load in the cerebrum and cerebellum appeared at 51 dpi (9.66×10^3 copies/ μ L, $P < 0.001$) and 46 dpi (2.40×10^6 copies/ μ L, $P < 0.001$), respectively (Fig. 1A, 1B). At that time, no clinical symptoms could be observed in the infected quails.

In the digestive system (proventriculus, intestine, liver and pancreas), the viral load in the proventriculus and intestine was higher than that in the nervous system. The time-related proliferation curve of the viral load in the proventriculus showed a "U-shape" from 3 dpi (8.91×10^4 copies/ μ L) to 46 dpi (1.04×10^6 copies/ μ L, $P < 0.001$). The viral load decreased from 46 dpi to 52 dpi (1.00×10^2 copies/ μ L, $P < 0.001$) and was then stable until 60 dpi (Fig. 1C). The time-related proliferation curve of the viral load in the intestine had an "M-shape" from 3 dpi to 46 dpi. One peak appeared at 20 dpi (2.63×10^7 copies/ μ L, $P < 0.001$) and another appeared at 36 dpi (2.29×10^6 copies/ μ L, $P < 0.001$), and then remained stable until 60 dpi (Fig. 1D). The curve of the viral load in the liver fluctuated sharply with the maximum viral load appearing at 52 dpi (2.11×10^4 copies/ μ L, $P < 0.001$) (Fig. 1E). The curve of the viral load in the pancreas was also M-shaped but the number of virus copies was always lower than the detectable limit (Fig. 1F).

In the spleen and bursa, the viral copy number was higher than that in the nervous system (Fig. 1G, 1H). The curve of the viral load in the spleen had a "W-shape" from 3 dpi (1.30×10^6 copies/ μ L) to 54 dpi (4.79×10^7 copies/ μ L, $P < 0.001$) and then decreased slowly until 60 dpi (4.47×10^5 copies/ μ L) (Fig. 1G). The curve of the viral load in the bursa was "U-shaped" from 3 dpi (6.92×10^6 copies/ μ L) to 44 dpi (9.77×10^7 copies/ μ L, $P < 0.001$), then decreased from 44 dpi to 49 dpi (4.62×10^3 copies/ μ L, $P < 0.001$) and then fluctuated from 49 dpi to 60 dpi (8.91×10^2 to 1.04×10^5 copies/ μ L) (Fig. 1H).

The curve of the viral copy number in the lung showed two "M shapes": one was from 3 dpi to 30 dpi and the other was from 30 dpi to 60 dpi. The two peaks of the first "M" appeared at 18 dpi (5.62×10^2 copies/ μ L, $P < 0.001$) and 29 dpi (1.08×10^3 copies/ μ L, $P < 0.001$) and the two peaks of the second "M" appeared at 46 dpi (1.70×10^4 copies/ μ L, $P < 0.001$) and 53 dpi (8.22×10^3 copies/ μ L, $P < 0.001$) (Fig. 1I). The curve of the viral load in the kidney had only one peak that appeared at 7 dpi (3.94×10^4 copies/ μ L, $P < 0.001$) and slightly fluctuated from 15 dpi to 60 dpi (Fig. 1J).

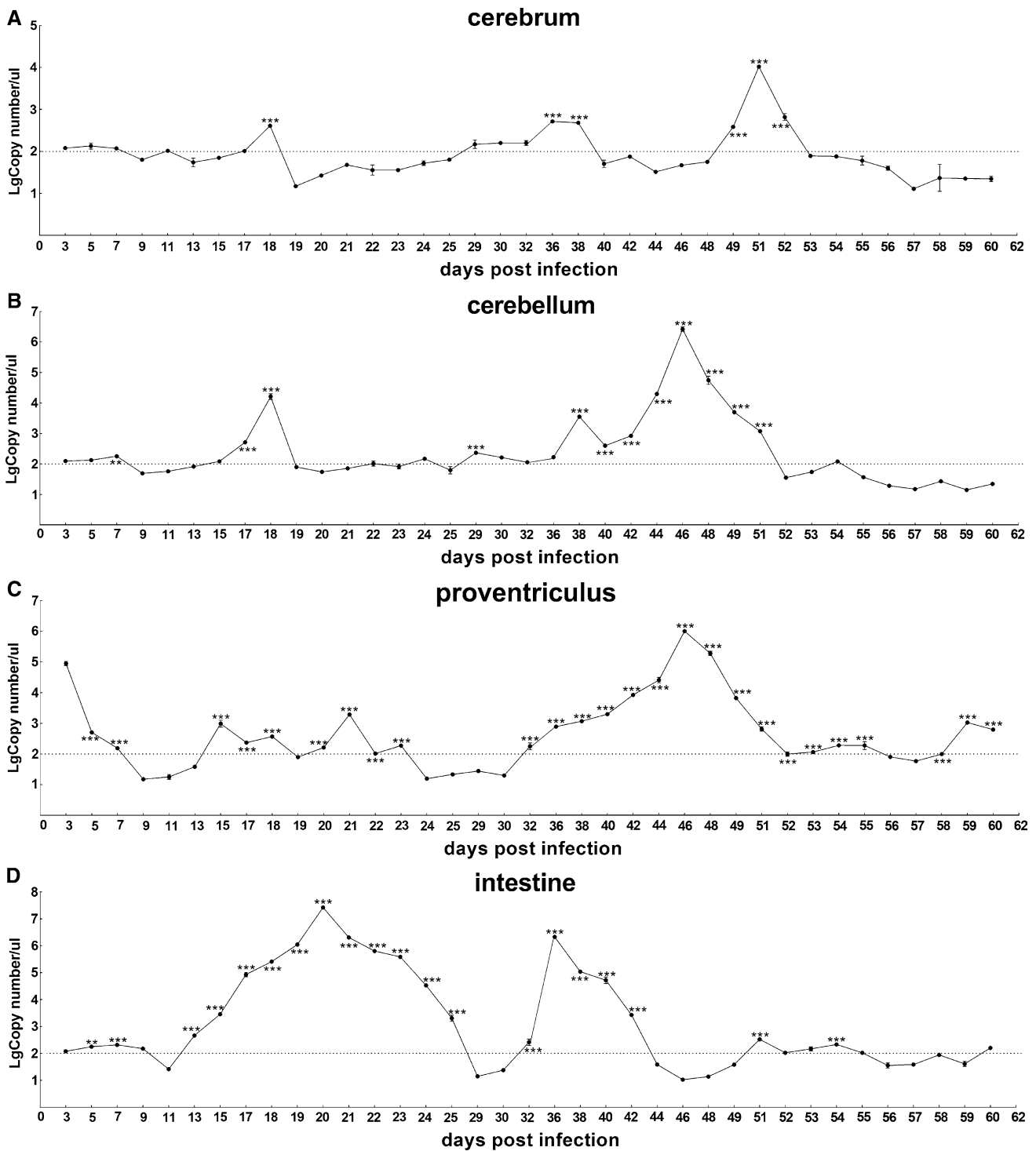


Fig. 1 The dynamic distribution of AEV in the cerebrum (A), cerebellum (B), proventriculus (C), intestine (D), liver (E), pancreas (F), spleen (G), bursa (H), lung (I) and kidney (J) of experimentally infected quails from 3 to 60 days post-infection (dpi). The viral load in each tissue was measured in triplicate using qPCR, then all values were converted to logarithm copies/ul. Significant differences in the

viral loads in the tissues between 3 dpi and other sampling times are indicated with two asterisks (**) for $P < 0.01$ or with three asterisks (***) for $P < 0.001$ using the one-way ANOVA test with Dunnett's T3 method. Samples with a copy number below the limit of detection (100 copies, dotted line) were regarded as negative and were not analyzed

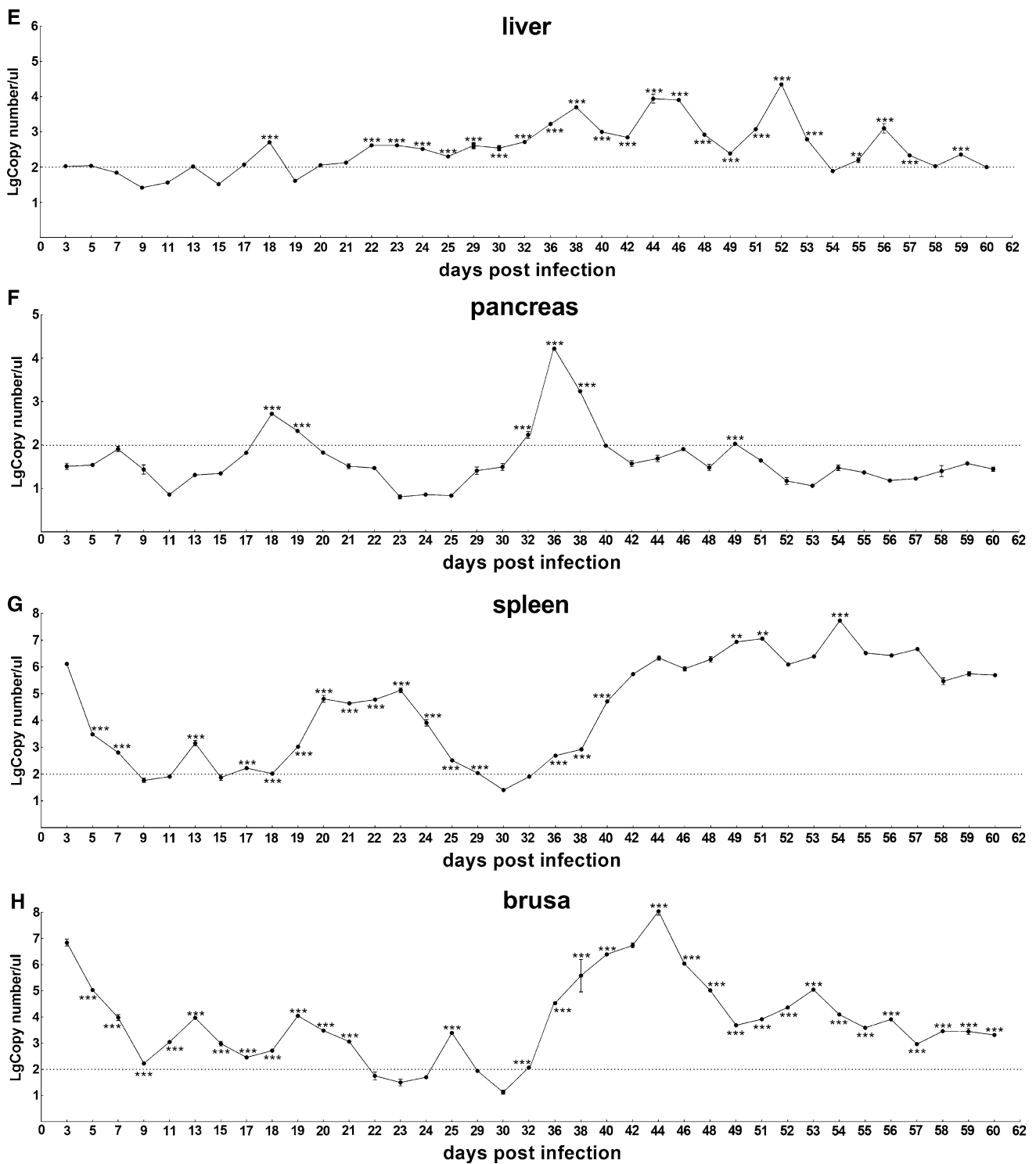


Fig. 1 (continued)

Analysis of AEV tissue distribution by IHC

The presence of positive staining signals for the AEV antigen in the sections was verified by IHC. All collected tissues from the infected quails showed clear positive staining and

the intensity was similar between the different repeats. The negative controls did not show any staining (Fig. 2). Vacuolated cells, which are characteristic of AEV lesions, were observed in the cerebrum and thus demonstrate that AEV not only replicated but also caused pathological lesions in

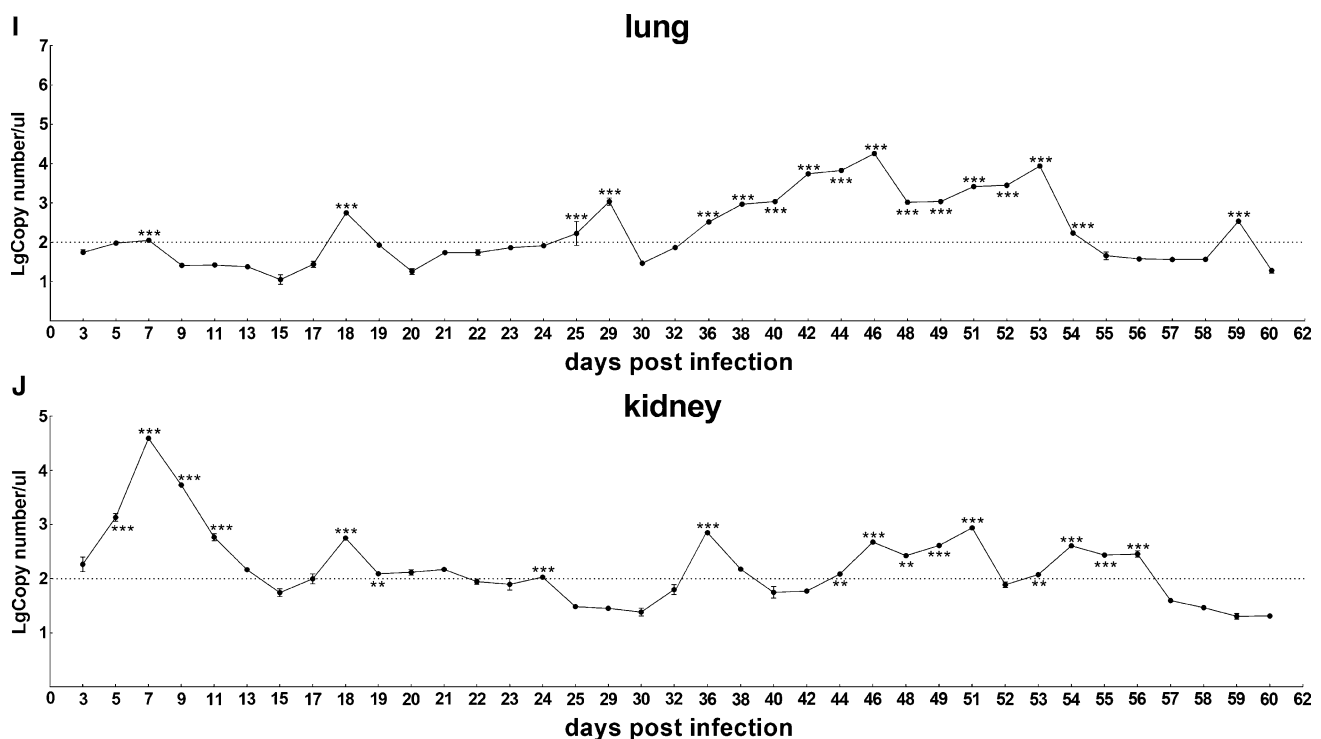


Fig. 1 (continued)

nerve cells (Fig. 2A). The positive staining signals surrounding the characteristic lesions were more obvious. The mean density values of each tissue at different dpi are presented in Table 1.

In the nervous system, the mean density had an “inverted V-shape” with the maximum values in the cerebrum and cerebellum appearing at 36 dpi (0.218, $P < 0.001$) and 18 dpi (0.211, $P < 0.001$), respectively.

In the digestive system, the mean densities of the proventriculus, liver and pancreas had an “N shape” with the maximum values appearing at 36 dpi (0.271, 0.188 and 0.192, respectively, $P < 0.001$). The mean density of the intestine was an inverted V-shape and the maximum value also appeared at 36 dpi.

In the immune system, the mean density was an “II-shape” with the maximum values in the spleen and bursa appearing at 54 dpi (0.203, $P < 0.01$) and 7 dpi, respectively.

The mean density in the lung was II-shaped with the maximum value appearing at 59 dpi. The mean density in the kidney was W-shaped with the maximum value appearing at 7 dpi.

The correlation analysis between the mean density (IHC) and the viral load (qPCR) at 7, 18, 36, 54 and 59 dpi in various tissues is presented in Table 2. There was a good correlation between the mean density and viral load in the cerebrum, cerebellum, intestine and liver and a positive

correlation in the proventriculus, pancreas, spleen, bursa, lung and kidney.

Discussion

AE is a contagious disease that causes enormous commercial losses in poultry throughout the world but the tissue distribution of the virus in quail remains unclear. In this study, 120 commercial one-day-old Korean quails were orally inoculated with AEV isolate XY/Q-1410.

According to our results, the associated morbidity was 30% and the mortality was 16.7%, which appears to be low and in contrast to clinical observations, possibly because of the virus titre used for the challenge as well as the route of inoculation [28]. The virus titre in the original homogenate of the AEV isolate XY/Q-1410 was $10^{-5.16}$, which was relatively low and imposed an upper limit for the challenge viral load. However, this low dose at viral challenge did ensure that enough quails survived for sampling late into the experiment. The quails were challenged orally, which may be another reason for the lower number of deaths. Hill and Raymond (1962) reported AE in quails by both natural infection and experimental infection [29]. They found that intracerebral inoculation of AEV killed one-day-old quails after a period of 16 days. In our experiment, orally infected

Fig. 2 Viral antigen located by immunohistochemistry (IHC) in various tissues. IHC staining in various tissues of experimentally infected Korean quails was observed. Positive AEV staining is shown in dark brown. Arrows indicate positive staining of viral antigens in various tissues: the cerebrum (A), cerebellum (B), proventriculus (C), intestine (D), liver (E), pancreas (F), spleen (G), bursa (H), lung (I) and kidney (J). (a–e): 7 dpi, 18 dpi, 36 dpi, 54 dpi, 59 dpi. f: Negative control. All scale bars represent 100 μm (400 \times magnification)

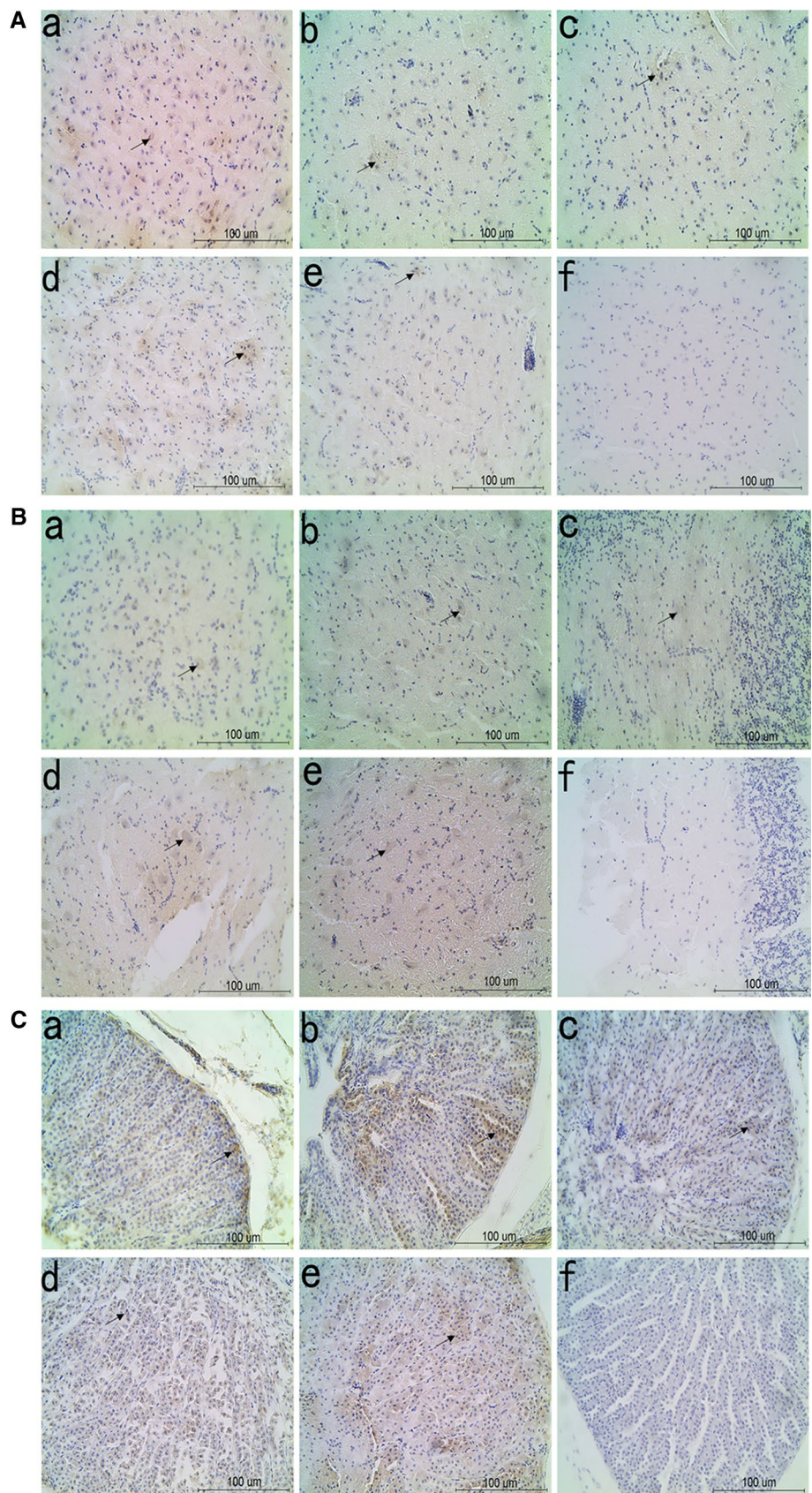


Fig. 2 (continued)

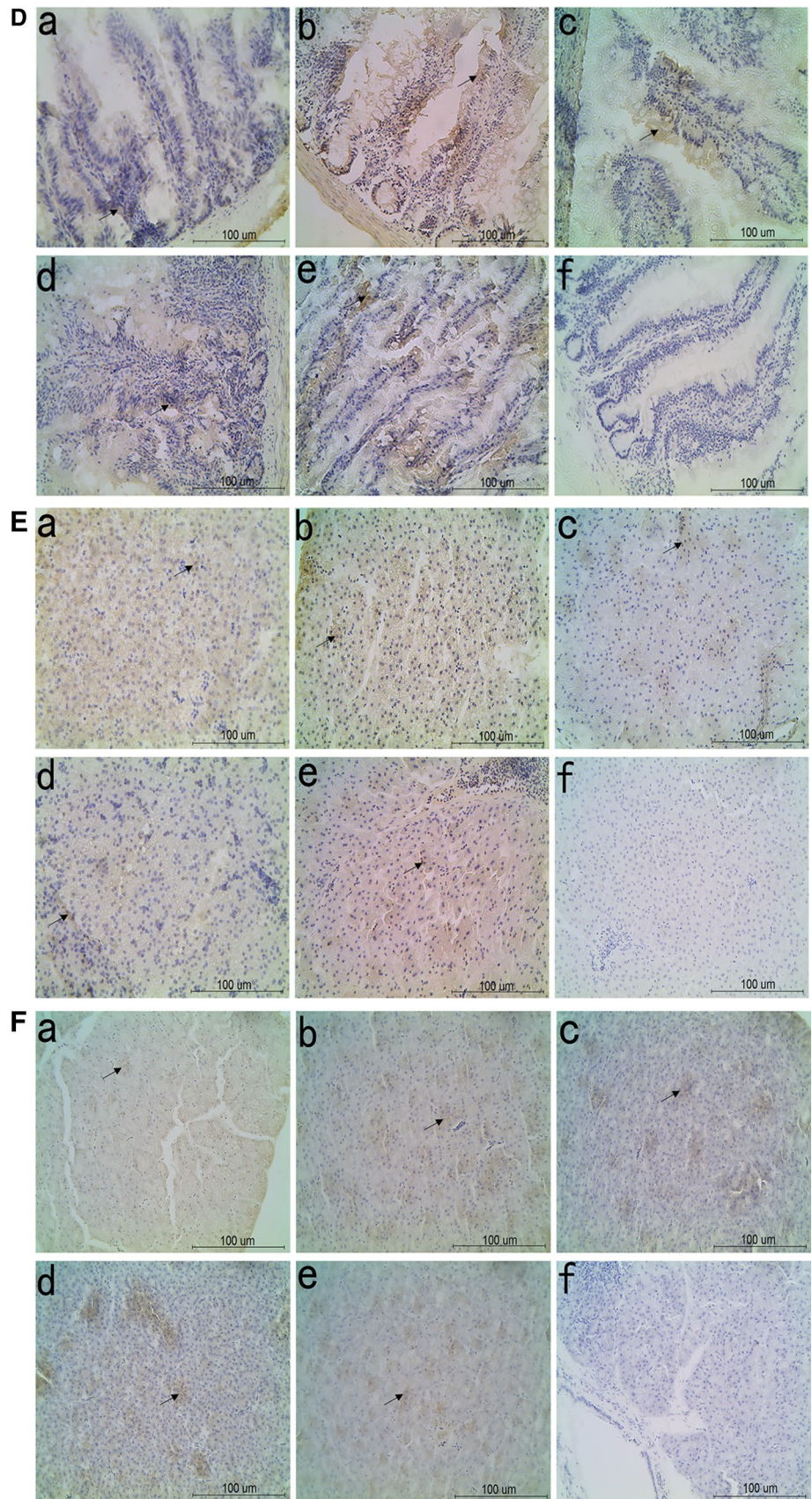


Fig. 2 (continued)

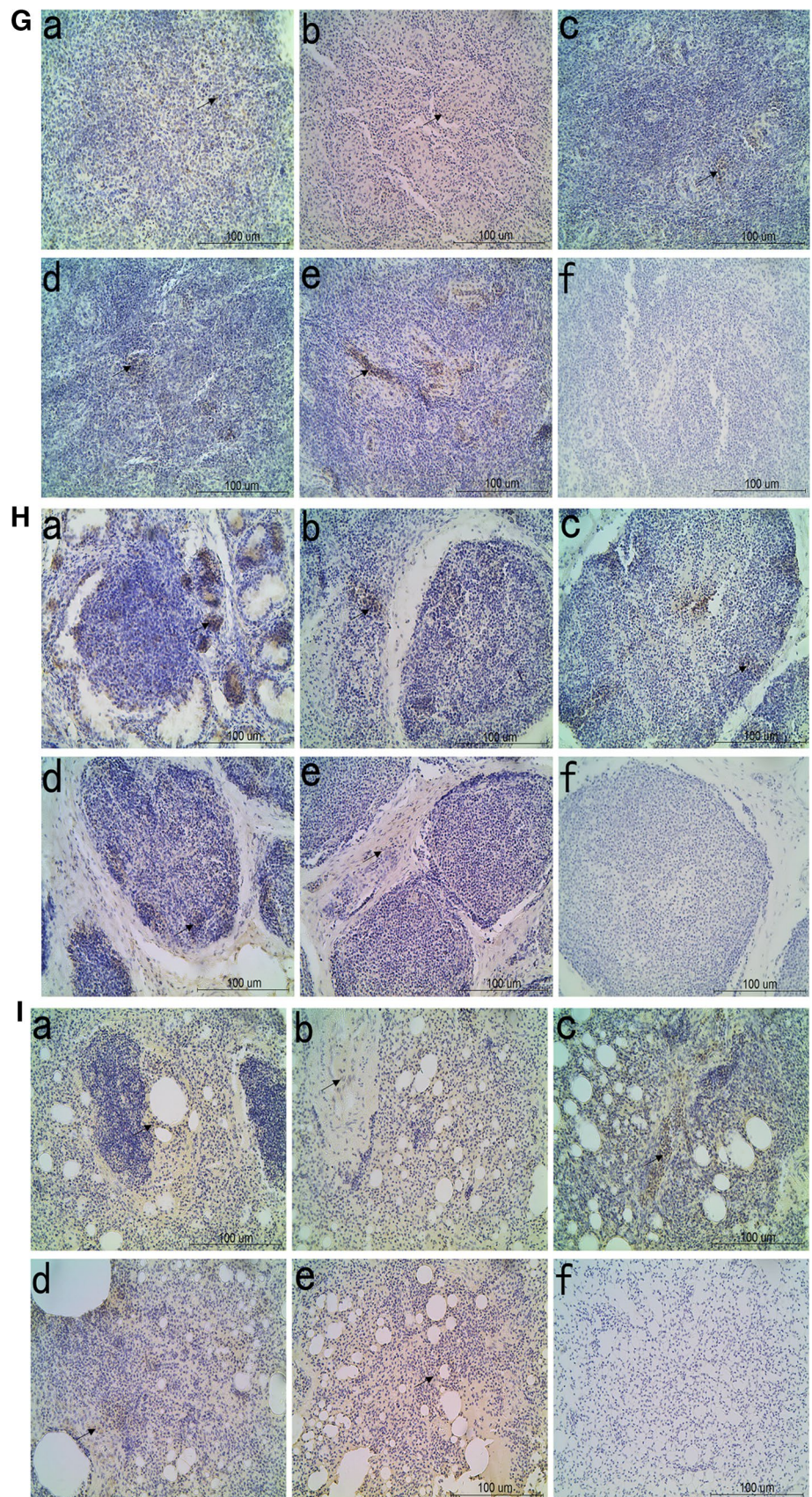
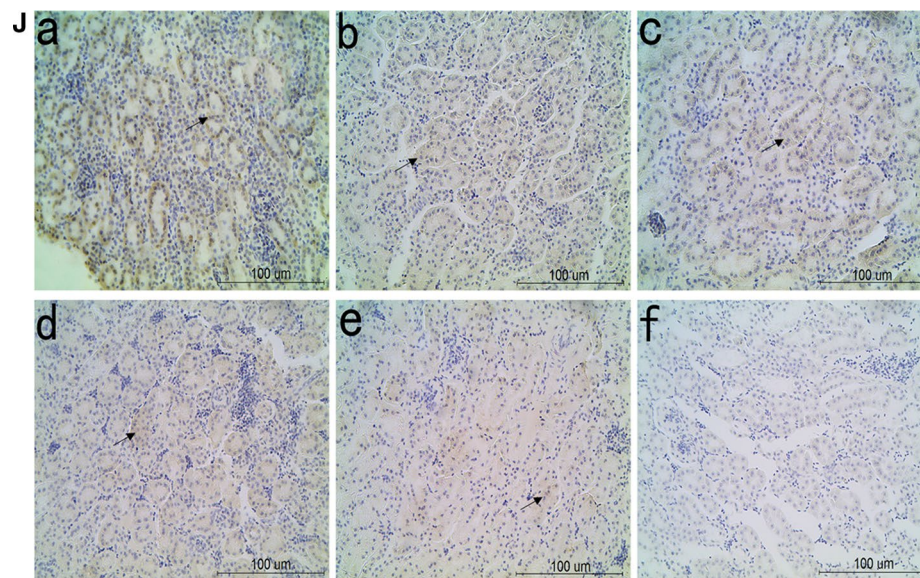


Fig. 2 (continued)**Table 1** Expression levels of viral antigen in various tissues by immunohistochemistry (IHC)

| Tissues | Density mean | | | | |
|----------------|---------------|---------------|---------------|---------------|---------------|
| | 7 dpi | 18 dpi | 36 dpi | 54 dpi | 59 dpi |
| Cerebrum | 0.166 ± 0.003 | 0.214 ± 0.021 | 0.218 ± 0.017 | 0.090 ± 0.001 | 0.085 ± 0.004 |
| Cerebellum | 0.182 ± 0.010 | 0.211 ± 0.008 | 0.168 ± 0.008 | 0.096 ± 0.005 | 0.080 ± 0.002 |
| Proventriculus | 0.177 ± 0.012 | 0.184 ± 0.006 | 0.217 ± 0.001 | 0.113 ± 0.004 | 0.165 ± 0.003 |
| Intestine | 0.191 ± 0.005 | 0.194 ± 0.002 | 0.225 ± 0.043 | 0.167 ± 0.008 | 0.150 ± 0.007 |
| Liver | 0.124 ± 0.007 | 0.155 ± 0.002 | 0.188 ± 0.021 | 0.136 ± 0.010 | 0.162 ± 0.002 |
| Pancreas | 0.125 ± 0.002 | 0.148 ± 0.002 | 0.192 ± 0.016 | 0.163 ± 0.003 | 0.170 ± 0.002 |
| Spleen | 0.135 ± 0.018 | 0.118 ± 0.019 | 0.173 ± 0.013 | 0.203 ± 0.026 | 0.117 ± 0.006 |
| Bursa | 0.176 ± 0.009 | 0.140 ± 0.006 | 0.157 ± 0.007 | 0.145 ± 0.006 | 0.140 ± 0.007 |
| Lung | 0.121 ± 0.004 | 0.127 ± 0.014 | 0.127 ± 0.002 | 0.111 ± 0.003 | 0.130 ± 0.013 |
| Kidney | 0.220 ± 0.009 | 0.081 ± 0.002 | 0.159 ± 0.006 | 0.085 ± 0.004 | 0.143 ± 0.012 |
| Control | – | – | – | – | – |

The mean density of AEV XY/Q-1410 staining in various tissues, including the cerebrum, cerebellum, proventriculus, intestine, liver, pancreas, spleen, bursa, lung and kidney at 7 dpi, 18 dpi, 36 dpi, 54 dpi and 59 dpi was determined using Image-Pro Plus 6.0. All values are presented as the mean ± SD. Significant differences in the mean density in the tissues between 3 dpi and samples at other dpi were analysed by SPSS 16.0

one-day-old quails died after a period of 18 days, which was 2 days later than for intracerebral inoculation.

To analyse AEV distribution in infected quails, qPCR and IHC were used in our experiment to quantify the viral load in different tissues. A SYBR Green-based absolute qPCR method was developed for rapid detection and quantification of AEV and was used for analysis of viral distribution in our previous research [4, 30, 31]. Here, the same detection system was used for analysis of the dynamic distribution and viral tissue tropism of AEV in artificially infected Korean quails. IHC has gained significance and is already a crucial tool for diagnosis of diseases and calculating prognosis for patients. IPP was used for quantitative in situ assessment of protein expression [32]. This application made improved

our IHC as well as reproducibility and accuracy. The mean signal density and IOD were representative parameters used for assessing immunostaining quantification. In addition the application of IPP improved our immunostaining quantification by increasing sensitivity in scoring and through providing a more reliable and reproducible analysis of protein expression [33].

We determined that the lowest detection limit of our qPCR was 100 viral copies. However, the fact that we routinely detected viral copies below this value does not mean the virus was cleared [1]. In contrast, IHC could detect the virus at a very low level. Thus, there may lower degrees of correlation between qPCR and IHC during low level virus replication. Furthermore, the viral replication cycle

Table 2 Correlation analysis between qPCR and IHC

| Tissues | Pearson correlation |
|----------------|---------------------|
| Cerebrum | 0.942 |
| Cerebellum | 0.816 |
| Proventriculus | 0.577 |
| Intestine | 0.869 |
| Liver | 0.938 |
| Pancreas | 0.520 |
| Spleen | 0.522 |
| Bursa | 0.552 |
| Lung | 0.663 |
| Kidney | 0.570 |
| Control | – |

Correlation analysis between qPCR and IHC in each tissue was performed by SPSS 16.0. The correlation coefficient (R^2) is represented by the Pearson correlation ($P < 0.05$)

consists of four consecutive steps: adsorption/penetration, shelling, biosynthesis, assemble and release. The viral RNA load detected by qPCR may not equal the number of virions. Therefore, it is reasonable to assume that the correlation between the qPCR and IHC was relatively poor in some tissues, such as the spleen.

In naturally infected chicks, the latency of AE is 10–30 days and the AE outbreak occurs mostly in 3-week-old chicks [34]. Virus shedding lasts from about 5 to 14 days however the virus shedding time could be extended if the birds were infected earlier [34]. In our experiment, the latency of the infected group was about 10 days and typical clinical symptoms (paralysis and tremors of the head and neck) appeared at 18 dpi, which is when the viral load in the cerebrum and cerebellum had reached its first peak. AEV may spread through vertical and horizontal routes; furthermore environmental virus in contaminated areas may remain infectious for a long time because of its great stability [1]. Further studies should be performed to determine the extent of AEV shedding and clearance times.

Over the course of our experiment, curves representing the viral load in various tissues of Korean quails were drawn and, according to these results, it was clear that AEV XY/Q-1410 could establish a persistent infection for up to 60 days. The viral load in the spleen and bursa remained at a relatively high level during this period. The viral load sharply fluctuated in the spleen and bursa, which indicates both active infection and an anti-viral response between the virus and the host. The viral loads in most tissues was relatively stable after 49 dpi, which indicated that a balance had been reached between the host and virus. Two peaks of viral load were observed in most tissues, possibly because of viraemia. As reported by Muir et al, viral replication leads to viraemia, which may produce a

second round of viral replication in tissues [35]. Cheville reported that the development of AE was inversely related to age in chicks [36]; since viral persistence in the brain and clinical symptoms were related to age when chickens were infected. Westbury and Sinkovic concluded that humoral immunity is the basis for age-related resistance [37]. Korean quail were cultivated from Japanese quail due to their physiological resemblance to chickens, as well as their resistance to diseases and natural resistance to infection with most of the viral infections affecting domestic poultry [38, 39]. Further studies correlating viral load, viraemia, antibody levels and the maturity of the immune system in experimentally infected quails could contribute to explaining the shape of the “viral replication curves” in the various tissues.

Different enteroviruses recognise different cell surface receptors and this partly determines the types of cell or tissue that can be infected. As a result enteroviruses vary markedly in their replication efficiency in various tissues [35]. We might speculate that viral load in the proventriculus, intestine, spleen and bursa was higher than in other tissues because there were more readily available receptors in these organs and thus AEV replicated more efficiently. Meanwhile, the higher viral load in the intestine indicates that the AEV strain XY/Q-1410 has an intestinal tropism.

In summary, we investigated the dynamic distribution of AEV in various tissues in experimentally infected Korean quails. Orally inoculated AEV killed one-day-old Korean quails after a period of 18 dpi and caused a persistent infection up to 60 days. Meanwhile, the viral load in the spleen and bursa remained at a relatively high level. Our study provides useful information for further research on the mechanisms underpinning the pathogenesis of AEV in quails and may also contribute to the further control of AE.

Acknowledgments This study was supported by the Agricultural Science and Technology Project of Shaanxi Province in China (Grant Number 2014K02-05-02).

Compliance with ethical standards

The animal experiment protocol complied with the Ethical Review Process and adhered to the guidelines of the Ethical and Animal Welfare Committee of Shaanxi Province, China.

Competing interests The authors declare that they have no competing interests.

References

1. Tannock GA, Shafren DR (1994) Avian encephalomyelitis: a review. *Avian Pathol* 23:603–620
2. Toplu N, Alçigir G (2004) Avian encephalomyelitis in naturally infected pigeons in Turkey. *Avian Pathol* 33:381–386

3. Welchman DdB, Cox WJ, Gough RE, Wood AM, Smyth VJ, Todd D, Spackman D (2009) Avian encephalomyelitis virus in reared pheasants: a case study. *Avian Pathol* 38:251–256
4. Liu Q, Yang Z, Hao H, Cheng S, Fan W, Du E, Xiao S, Wang X, Zhang S (2014) Development of a SYBR Green real-time RT-PCR assay for the detection of avian encephalomyelitis virus. *J Virol Methods* 206:46–50
5. Taylor LW, Lowry DC, Raggi LG (1955) Effects of an outbreak of avian encephalomyelitis (epidemic tremor) in a breeding flock. *Poult Sci* 34:1036–1045
6. Berger RG (1982) An in vitro assay for quantifying the virus of avian encephalomyelitis. *Avian Dis* 26:534–541
7. Meroz M, Elkin N, Hadash D, Abrams M (1990) Egg drop associated with avian encephalomyelitis virus. *Vet Rec* 127:532
8. Yu XH, Zhao J, Qin XH, Zhang GZ (2015) Serological evidence of avian encephalomyelitis virus infection associated with vertical transmission in chicks. *Biologicals* 43:512–514
9. Marvil P, Knowles NJ, Mockett AP, Britton P, Brown TD, Cavanagh D (1999) Avian encephalomyelitis virus is a picornavirus and is most closely related to hepatitis A virus. *J Gen Virol* 80(Pt 3):653–662
10. Adams MJ, Carstens EB (2014) Ratification vote on taxonomic proposals to the International Committee on Taxonomy of Viruses (2014). *Arch Virol* 157:1411–1422
11. Mancini LO, Yates VJ (1967) Cultivation of avian encephalomyelitis virus in vitro. 1. In chick embryo neuroglial cell culture. *Avian Dis* 11:672–679
12. Mancini LO, Yates VJ (1968) Cultivation of avian encephalomyelitis virus in vitro. 2. In chick embryo fibroblastic cell culture. *Avian Dis* 12:278–284
13. Mancini LO, Yates VJ (1968) Research note: cultivation of avian encephalomyelitis virus in chicken embryo kidney cell culture. *Avian Dis* 12:686–688
14. Sumner FW, Luginbuhl RE, Jungherr EL (1957) Studies on avian encephalomyelitis. II. Flock survey for embryo susceptibility to the virus. *Am J Vet Res* 18:720
15. Calnek BW, Jehnich H (1959) Studies on Avian Encephalomyelitis. I. The use of a serum-neutralization test in the detection of immunity levels. *Avian Dis* 3(2):95–104
16. Lukert PD, Davis RB (1971) An antigen used in the agar-gel precipitin reaction to detect avian encephalomyelitis virus antibodies. *Avian Dis* 15:935–938
17. Miyamae T (1974) Ecological survey by the immunofluorescent method of virus in enzootics of avian encephalomyelitis. *Avian Dis* 18(3):369–377
18. Miyamae T (1977) Immunofluorescent study on egg-adapted avian encephalomyelitis virus infection in chickens. *Am J Vet Res* 38:2009–2012
19. Ahmed AA, Elazm IM, Ayoub NN, Eltoukhi BI (1982) Studies on the serological detection of antibodies to avian encephalomyelitis virus. *Avian Pathol* 11:253–262
20. Braune MO, Gentry RF (1971) Avian encephalomyelitis virus. I. Pathogenesis in chicken embryos. *Avian Dis* 15(4):648–653
21. Ikeda S, Matsuda K (1976) Susceptibility of chickens to avian encephalomyelitis virus. V. Behavior of a field strain in laying hens. *Natl Inst Anim Health Q* 16:90–96
22. Wang Z, Liu H, Jiangtao XU, Bao J, Zheng D, Sun C, Wei R, Song C, Chen J (2006) Genotyping of newcastle disease viruses isolated from 2002 to 2004 in China. *Ann N Y Acad Sci* 1081:228–239
23. OIE (Office International des Epizooties) (2008) Avian infectious bronchitis. Manual of diagnostic tests and vaccines for terrestrial animals 2008 (pp. 435–455). Part 2, Section 2.3, Chapter 2.3.2. Retrieved from http://web.oie.int/eng/normes/MANUAL/2008/pdf/2.03.02_AIB.pdf. Accessed 17 July 2008
24. Peiris M, Yam WC, Chan KH, Ghose P, Shortridge KF (1999) Influenza A H9N2: aspects of laboratory diagnosis. *J Clin Microbiol* 37(10):3426–3427
25. Reed LJ, Muench H (1938) A simple method of estimating fifty per cent endpoints. *Am J Epidemiol* 27(3):493–497
26. Chaves AJ, Busquets N, Valle R, Rivas R, Vergaraalert J, Dolz R, Ramis A, Darji A, Majó N (2011) Neuropathogenesis of a highly pathogenic avian influenza virus (H7N1) in experimentally infected chickens. *Vet Res* 42:1–13
27. Xavier LL, Viola GG, Ferraz AC, Da CC, Deonizio JM, Netto CA, Achaval M (2005) A simple and fast densitometric method for the analysis of tyrosine hydroxylase immunoreactivity in the substantia nigra pars compacta and in the ventral tegmental area. *Brain Res Protoc* 16:58–64
28. Oladele OO, Esan OO, Jubril A, Jarikre T (2014) Presumptive diagnosis of avian encephalomyelitis in Japanese quail in Ibadan, Nigeria. *Bull Anim Health Prod Afr* 62(2):243–246
29. Hill RW, Raymond RG (1962) Apparent natural infection of coturnix quail hens with the virus of avian encephalomyelitis: case report. *Avian Dis* 6:226–227
30. Agarwal A, Singh AK, Sharma S, Soni M, Thakur AK, Gopalan N, Parida MM, Rao PV, Dash PK (2013) Application of real-time RT-PCR in vector surveillance and assessment of replication kinetics of an emerging novel ECSA genotype of Chikungunya virus in *Aedes aegypti*. *J Virol Methods* 193:419–425
31. Wang LG, Ma J, Xue CY, Wang W, Guo C, Chen F, Qin JP, Huang NH, Bi YZ, Cao YC (2013) Dynamic distribution and tissue tropism of infectious laryngotracheitis virus in experimentally infected chickens. *Arch Virol* 158:659–666
32. Cregger M, Berger AJ, Rimm DL (2006) Immunohistochemistry and quantitative analysis of protein expression. *Arch Pathol Lab Med* 130:1026–1030
33. Wang CJ, Zhou ZG, Holmqvist A, Zhang H, Li Y, Adell G, Sun XF (2009) Survivin expression quantified by Image Pro-Plus compared with visual assessment. *Appl Immunohistochem Mol Morphol Aimm* 17:530–535
34. Chen FY (2006) Veterinary immunology, 5th edn. China Agriculture Press, Beijing, pp 373–375
35. Muir P (2014) Enteroviruses. *Medicine* 42:57–59
36. Chevillat NF (1970) The influence of thymic and bursal lymphoid systems in the pathogenesis of avian encephalomyelitis. *Am J Pathol* 58:105–125
37. Westbury HA, Sinkovic B (1978) The pathogenesis of infectious avian encephalomyelitis. *Aust Vet J* 54:68–71
38. Ratnamohan N (1985) The management of Japanese quail and their use in virological research: a review. *Vet Res Commun* 9:1–14
39. Vali N (2008) The Japanese quail: a review. *Int J Poult Sci* 7:925–931